Diastereoselective Synthesis of the Indenylruthenium(II) Complexes [Ru(η^5-C_9H_7){κ^3(*P*,*C*,*C*)-$Ph_2P(CH_2CR{=}CH_2)$}(PPh_3)][PF_6] (R = H, Me): Enantiofacial Coordination, Hemilabile Properties, and Diastereoselective Nucleophilic Additions to κ^3(*P*,*C*,*C*)-Allylphosphine Ligands

Patricia Álvarez,[†] Elena Lastra,[†] José Gimeno,*[,†] Pedro Braña,[‡] José A. Sordo,[‡] Julio Gomez,[§] Larry R. Falvello,[∥] and Mauro Bassetti[⊥]

Departamento de Química Orgánica e Inorgánica, Instituto de Química Organometálica "Enrique Moles" (Unidad Asociada al CSIC), and Laboratorio de Química Computacional, Departamento de Química Física y Analítica, Universidad de Oviedo, Oviedo, Principado de Asturias, Spain, Department of Chemistry, Universidad de La Rioja, Complejo Científico Tecnológico, Calle Madre de Dios, 51, 26006 Logroño, Spain, Departamento de Química Inorgánica, Facultad de Ciencias, Universidad de Zaragoza-CSIC, E-50009 Zaragoza, Spain, and Istituto CNR di Metodologie Chimiche, Sezione Meccanismi di Reazione, and Dipartimento di Chimica, Università "La Sapienza", 00185 Roma, Italy

Received January 8, 2004

The mixed-phosphine complexes [Ru(η^5-C_9H_7)Cl{κ^1(*P*)-$Ph_2P(CH_2CR{=}CH_2)$}(PPh_3)] (R = H (**1a**), Me (**1b**)) are prepared by phosphine exchange reactions (1:1 molar ratio) of [Ru(η^5-C_9H_7)Cl(PPh_3)$_2$] with the corresponding allylphosphines $Ph_2P(CH_2CR{=}CH_2)$ in refluxing THF. The reaction of **1a** with sodium methoxide in methanol yields the hydride derivative [Ru(η^5-C_9H_7)H{κ^1(*P*)-$Ph_2P(CH_2CH{=}CH_2)$}(PPh_3)] (**1c**). The treatment of complexes **1a** and **1b** with $NaPF_6$ in methanol diastereoselectively affords the cationic complexes [Ru(η^5-C_9H_7)-{κ^3(*P*,*C*,*C*)-$Ph_2P(CH_2CR{=}CH_2)$}(PPh_3)][PF_6] (R = H (**2a**), Me (**2b**)) in good yield. An X-ray crystal structure determination of complex **2a** shows that the *si* enantiofacial coordination of the olefin group accompanies the *R* relative configuration of the metal center. No epimerization process has been observed. Olefin exchange substitution reactions of complex **2a** with MeCN and BzCN (1:1.5 molar ratio) in refluxing CH_2Cl_2 yield the cationic complexes [Ru(η^5-C_9H_7)(NCR){κ^1(*P*)-$Ph_2P(CH_2CH{=}CH_2)$}(PPh_3)][PF_6] (R = Me (**3a**), Bz (**3b**)). Similarly, the neutral complexes [Ru(η^5-C_9H_7)(N_3){κ^1(*P*)-$Ph_2P(CH_2CR{=}CH_2)$}(PPh_3)] (R = H (**4a**), Me (**4b**)) are obtained by the treatment of complexes **2a**,**b** with sodium azide in THF/MeOH at room temperature. The addition of lithium carbanions LiR′ (R′ = Me, *n*Bu) to solutions of complexes **2a**,**b** in tetrahydrofuran results in regio- and stereoselective exo addition at the C_β atom of the coordinated allylic group, affording the ruthenacyclopentane complexes [Ru(η^5-C_9H_7){κ^2(*P*,*C*)-$Ph_2P\{CH_2C(R)(R')CH_2\}$}($PPh_3$)] (R = H, R′ = Me (**5a**), *n*Bu (**5b**); R = Me, R′ = Me (**6a**), *n*Bu (**6b**)) in 80−95% yield. Similarly, the complexes [Ru(η^5-C_9H_7){κ^2(*P*,*C*)-$Ph_2P\{CH_2CH(R)CH_2\}$}(PPh_3)] (R = H (**5c**), Me (**6c**)) are formed by the reaction of equimolar mixtures of complexes **2a**,**b** with Li[$B(C_2H_5)_3H$]. The molecular structure and relative configurations $R_{Ru}S/S_{Ru}R$ of the new stereogenic atoms of complex **5b** have been determined by X-ray diffraction. Kinetic studies on the substitution reaction of complex **2a** with CD_3CN in $CDCl_3$ indicate that the olefin exchange occurs via parallel first-order (dissociative) and second-order (associative) pathways and highlight the intermediacy of a transient coordinatively unsaturated species, formed by olefin dissociation before attack of the nitrile.

Introduction

Prochiral alkenes are among the most common starting materials for enantioselective synthesis. Reaction methodologies involve transition-metal fragments which either bear a chiral center or activate the substrate toward the addition of a nucleophile in a stereoselective manner. In particular, monosubstituted alkenes (RCH=CH_2) and unsymmetrically substituted geminal alkenes (R(R′)C=CH_2), bearing different C=C termini substituents, feature binding modes that can give two enantiotopic faces upon coordination to a metal center (configurational diastereomers A and B: Chart 1). Moreover, providing that rotation around the C=C π bond is

[†] Departamento de Química Orgánica e Inorgánica, Universidad de Oviedo.
[‡] Departamento de Química Física y Analítica, Universidad de Oviedo.
[§] Universidad de La Rioja.
[∥] Universidad de Zaragoza-CSIC.
[⊥] CNR, Instituto di Metodologie Chimiche.

10.1021/om040001q CCC: $27.50
Publication on Web 05/11/2004

Chart 1

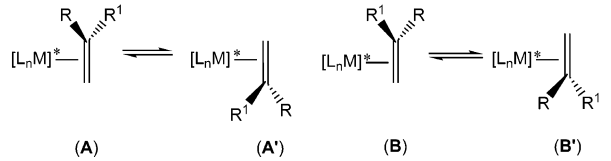

Chart 2

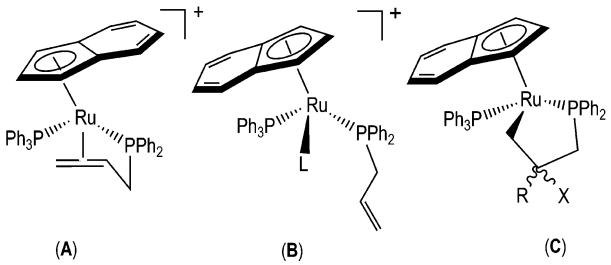

allowed, two M−(C═C) rotamers can exist for each of the two isomers (A′ and B′). As a result, a new stereogenic carbon atom is generated, giving rise to chiral complexes which normally are formed in equal amounts.

The use of chiral or prochiral metal fragments provides the most direct means of chiral recognition of these alkenes, enabling their potential enantioface binding selectivities. To fulfill this goal, considerable effort has been devoted to the design of organo transition-metal complexes with appropriate electronic and steric properties,[1] which would promote high binding selectivities. During the past few years we have extensively studied the chemistry of indenylruthenium(II) bis(phosphine) complexes [RuX(η^5-C_9H_7)$(L)_2$] and investigated the steric influence of the indenyl ring and of the ancillary ligands in the selectivity of both stoichiometric[2] and catalytic transformations.[3]

In this paper we report the stereoselective synthesis and reactivity of the mixed-phosphine complexes [Ru(η^5-C_9H_7)$(PPh_3)\{\kappa^3(P,C,C)$-$PPh_2(CH_2CR{=}CH_2)\}$][PF_6] (R = H, Me) bearing the hybrid hemilabile ligand allyldiphenylphosphine, which provides a coordinated olefin group attached to a chiral metal fragment (A in Chart 2). The enantiofacial binding ability of the indenylruthenium fragment with respect to the π-olefin group prompted us to explore the selectivity of the enantiotopic nucleophilic additions. The hemilabile properties of the allylphosphine ligand raise the question of whether a competition between olefin−nucleophile exchange (B in Chart 2) and nucleophilic addition (C in Chart 2) can occur. As is well-known, this is the main drawback in studies of the reactivity of olefin complexes.

Scheme 1[a]

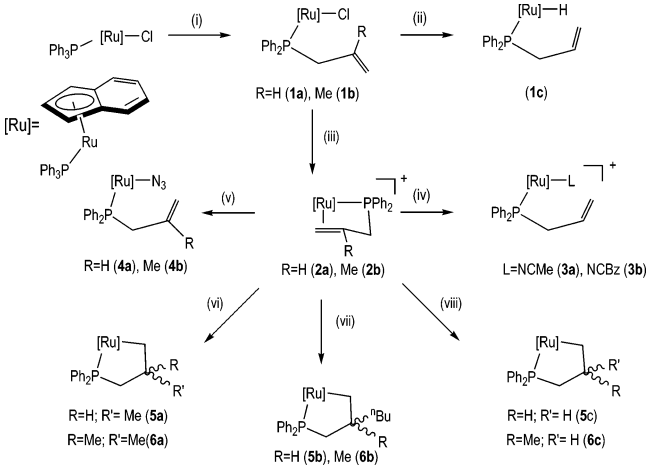

[a] Absolute configurations are not noted. Legend: (i) Ph_2PCH_2-CR═CH_2, THF reflux, 15 min; (ii) NaOMe, MeOH reflux, 30 min; (iii) $NaPF_6$, MeOH reflux, 30 min; (iv) 1.5 RCN, CH_2Cl_2 reflux, 45 min; (v) NaN_3, THF/MeOH, room temperature, 30 min; (vi) MeLi, THF, room temperature, 10 min; (vii) *n*BuLi, THF, room temperature, 10 min; (viii) Li[$B(C_2H_2)_3H$], THF, room temperature, 10 min.

Results and Discussion

Scheme 1 details the syntheses of the new complexes.

Synthesis of the Precursor Complexes [Ru(η^5-C_9H_7)X$\{\kappa^1(P)$-$Ph_2P(CH_2CR{=}CH_2)\}(PPh_3)$] (X = Cl, R = H (1a), Me (1b); X = H, R = H (1c)). The chloride mixed-phosphine complexes [Ru(η^5-C_9H_7)Cl$\{\kappa^1(P)$-$Ph_2P(CH_2CR{=}CH_2)\}(PPh_3)$] (R = H (**1a**), Me (**1b**)) are obtained via a phosphine exchange reaction by treatment of [Ru(η^5-C_9H_7)Cl$(PPh_3)_2$] with 1 equiv of allyldiphenylphosphines $Ph_2PCH_2CR{=}CH_2$ (R = H, Me) in refluxing THF for 10 min. They have been isolated as air-stable red solids in 85% yield (Scheme 1).[4] Elemental analysis and NMR spectroscopic data (^{1}H, ^{31}P{^{1}H}, ^{13}C{^{1}H}) of **1a**,**b** are in accord with the proposed formulations. The ^{31}P{^{1}H} NMR spectra show two doublet resonances at δ 48.0 and 45.3 (d, J_{PP} = 43.0 Hz) for **1a** and at δ 48.8 and 45.5 (J_{PP} = 42.2 Hz) for **1b**, in accord with the expected AB system arising from the presence of inequivalent phosphorus nuclei in the two monodentate phosphines. ^{1}H and ^{13}C{^{1}H} NMR spectra confirm the κ(P) coordination mode of the allylphosphines, displaying resonances of the noncoordinated allyl groups. The most significant features are as follows: (i) in the ^{1}H NMR spectra, two ═CH_2 resonances at δ 3.03 (br s), 4.92 (m) (**1a**) and δ 2.94 (s), 4.28 (s) (**1b**) and one CH at δ 4.87 (m) (**1a**) and Me at δ 0.89 (s) (**1b**); (ii) in the ^{13}C{^{1}H} NMR spectra, the resonances of olefinic carbons ═CH_2 at δ 119.8 (d, J_{CP} = 8.5 Hz) (**1a**) and 115.2 (d, J_{CP} = 7.5 Hz) (**1b**) and ═CR at δ 128.1 (s br) (**1a**) and δ 140.1 (d, J_{CP} = 13.9 Hz) (**1b**).

The hydride complex [Ru(η^5-C_9H_7)H$\{\kappa^1(P)$-$Ph_2P(CH_2$-CH═$CH_2)\}(PPh_3)$] (**1c**) is obtained (80%) by treatment of **1a** with NaOMe/MeOH in refluxing MeOH. Complex **1c** is isolated as an air-stable crystalline solid and has been characterized by analytical and spectroscopic means (see Experimental Section for details). In particular the ^{1}H NMR spectrum shows the hydride reso-

(1) Gladysz, J. A.; Boone, B. I. *Angew. Chem., Int. Ed. Engl.* **1997**, *36*, 550.

(2) Regio- and stereoselective nucleophilic additions to unsaturated carbenes have been reported. For recent publications see for example: (a) Cadierno, V.; Conejero, S.; Gamasa, M. P.; Gimeno, J.; Falvello, L. R.; Llusar, R. M. *Organometallics* **2002**, *21*, 3716. (b) Cadierno, V.; Gamasa, M. P.; Gimeno, J.; Perez-Carreño, E.; García-Granda, S. *J. Organomet. Chem.* **2003**, *670*, 75.

(3) (i) Dimerization of terminal alkynes: (a) Bassetti, M.; Marini, S.; Tortorella, F.; Cadierno, V.; Diez, J.; Gamasa, M. P.; Gimeno, J. *J. Organomet. Chem.* **2000**, *593*−*594*, 292. (b) Bassetti, M.; Marini, S.; Diez, J.; Gamasa, M. P.; Gimeno, J.; Rodríguez-Alvarez, Y.; García-Granda, S. *Organometallics* **2002**, *21*, 4815. (ii) Hydration of alkynes: (c) Alvarez, P.; Gimeno, J.; Lastra, E.; García-Granda, S.; Van der Maelen, J. F.; Bassetti, M. *Organometallics* **2001**, *20*, 3762. (d) Alvarez, P.; Gimeno, J.; Bassetti, M.; Mancini, G. *Tetrahedron Lett.* **2001**, *42*, 8467. (iii) Polymerization processes: (e) Alvarez, P.; Gimeno, J.; Lastra, E. *Organometallics* **2002**, *21*, 5678.

(4) A longer reaction time leads to the simultaneous formation of the bis-substituted complexes [Ru(η^5-C_9H_7)Cl$\{\kappa^1(P)$-$Ph_2P(CH_2CR{=}CH_2)\}_2$]: Unpublished results.

nance as a virtual triplet (δ −15.32, $^2J_{HP}$ = 31.9 Hz), which compares well with those shown by the analogous indenyl complexes [Ru(η^5-C_9H_7)HL_2] in the range δ −14.12 to −17.07.[5] The $^{31}P\{^1H\}$ NMR spectrum shows two doublet resonances at δ 62.2 and 53.3 (J_{PP} = 25.9 Hz), in agreement with the expected AB pattern.

κ^3(*P,C,C*)-Allylphosphine Complexes [Ru(η^5-C_9H_7){κ^3(*P,C,C*)-$Ph_2P(CH_2CR{=}CH_2)$}(PPh_3)][PF_6] (R = H (2a), Me (2b)). Treatment of a solution of either of the chloride complexes **1a** and **1b** in refluxing methanol with 1 equiv of $NaPF_6$ for 30 min gives a yellowish solution from which the cationic complexes [Ru(η^5-C_9H_7){κ^3(*P,C,C*)-$Ph_2P(CH_2CR{=}CH_2)$}(PPh_3)]-[PF_6] (R = H (**2a**), Me (**2b**)) are isolated as air-stable yellow hexafluorophosphate salts (90%) (Scheme 1). The products have been characterized by elemental analyses and NMR data, which confirm the coordination mode of the allyl phosphine as κ^3(P,C,C). In particular, the ^1H and $^{13}C\{^1H\}$ NMR spectra show CR=CH_2 (R = H, Me) resonances which appear at higher field than those observed in complexes **1a**−**c**, bearing a noncoordinated olefinic system κ^1(*P*) (see Experimental Section). $^{31}P\{^1H\}$ NMR spectra at room temperature also reveal the effect of the olefin coordination, showing the expected resonances for an AB system with the signals for the allylphosphine shifted toward higher field at δ 55.2 and −69.9 (J_{PP} = 36.6 Hz) (**2a**) and δ 51.4 and −63.9 (J_{PP} = 34.5 Hz) (**2b**) with respect to those of the corresponding κ^1(*P*) precursors[6] (see Experimental Section). Since the two olefin faces of the κ^1(*P*)-$Ph_2P(CH_2CR{=}CH_2)$ (R = H, Me) ligand in complexes **1a**,**b** are diastereotopic,[1,7] the formation of only one isomer for each of the complexes **2a**,**b** indicates that the generation of the chelate ring [Ru{κ^3(*P,C,C*)-$Ph_2P(CH_2CR{=}CH_2)$}] proceeds in a highly diastereoselective manner. The relatively large difference of geminal CH_2 chemical shifts in ^1H NMR spectra points to a parallel orientation of the olefin with respect to the indenyl ring. Similar data have been reported in cyclopentadienyl and indenyl π-olefin complexes.[8] It is interesting to note that the $^{31}P\{^1H\}$ NMR spectra in acetone remain unchanged within a wide range of temperature (−90 to +50 °C), obviating the possibility of a dynamic process involving an equilibrium between the two diastereomers. No epimerization is observed in solution within 96 h. These results contrast with those reported for the analogous complex [Ru(η^5-C_5Me_5){κ^1(*P*)-$Ph_2PCH_2CH{=}CH_2$}{κ^3(*P,C,C*)-$Ph_2PCH_2CH{=}CH_2$}][PF_6],[9a] which is fluxional, giving rise to a rapid equilibrium between the two diastereomers on the NMR time scale.[10]

To find out which of the two enantiotopic olefin faces in the κ^1(*P*)-$Ph_2P(CH_2CR{=}CH_2)$ ligand is most favored for coordination, the structure of complex **2a** has been determined by X-ray crystallography. Suitable crystals were obtained by slow diffusion of diethyl ether into a solution of complex **2a** in CH_2Cl_2. An ORTEP representation is shown in Figure 1, and selected bonding data are collected in the caption.

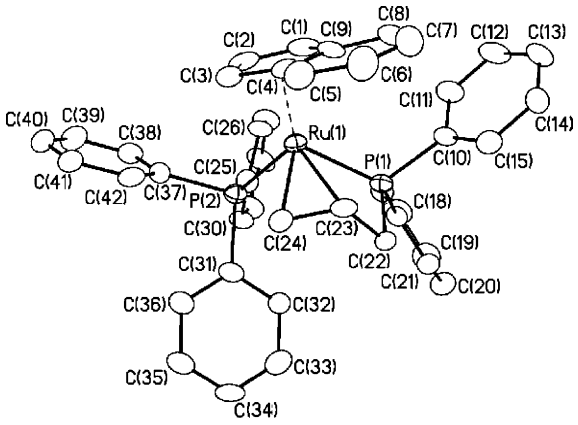

Figure 1. Molecular structure and atom-labeling scheme for complex **2a**. Non-hydrogen atoms are represented by their 50% probability ellipsoids. Hydrogen atoms have been omitted for clarity. Selected bond lengths (Å): Ru(1)−C* = 1.910(3), Ru(1)−P(1) = 2.3416(17), Ru(1)−P(2) = 2.3078-(17), Ru(1)−C(23) = 2.228(5), Ru(1)−C(24) = 2.243(5), P(1)−C(22) = 1.812(6), C(22)−C(23) = 1.519(8), C(23)−C(24) = 1.391(8). Selected bond angles (deg): C*−Ru(1)−P(1) = 128.89(12), C*−Ru(1)−P(2) = 120.92(11), C*−Ru(1)−C(23) = 121.57(18), C*−Ru(1)−C(24) = 120.29(19), P(1)−Ru(1)−P(2) = 96.09(6), P(1)−Ru(1)−C(23) = 65.14-(15), P(1)−Ru(1)−C(24) = 93.70(15), P(2)−Ru(1)−C(23) = 110.55(16), P(2)−Ru(1)−C(24) = 86.51(16), C(23)−Ru(1)−C(24) = 36.2(2), Ru(1)−P(1)−C(22) = 90.81(19), P(1)−C(22)−C(23) = 94.9(3), C(22)−C(23)−C(24) = 123.8(5), Ru(1)−C(24)−C(23) = 71.3(3). C* = centroid of the indenyl ligand.

The molecule exhibits a pseudooctahedral three-legged piano-stool geometry with the η^5-indenyl ligand displaying the usual allylene coordination mode. The interligand angles P(1)−Ru(1)−P(2), P(1)−Ru(1)−C(24), and P(2)−Ru(1)−C(23) and those between the five-membered-ring centroid C* and the legs, namely P(2)−Ru(1)−C*, C(24)−Ru(1)−C*, C(23)−Ru(1)−C*, and P(1)−Ru(1)−C*, show values typical of a pseudooctahedron (see the caption to Figure 1). The Ru−C(23) and Ru−C(24) bond distances reflect the coordination of the olefin to the metal center, and the C(23)−C(24) bond distance, 1.391(8) Å, is similar to those in the complex [Ru(η^5-C_5Me_5){κ^1(*P*)-$Ph_2P(CH_2CH{=}CH_2)$}{κ^3(*P,C,C*)-$Ph_2P(CH_2CH{=}CH_2)$}][PF_6].[9a] It is also interesting to note that the benzo ring of the indenyl ligand is oriented over the olefin ligand, slightly displaced toward P(1). Both enantiomers are present in equal proportion in the crystal, which belongs to a centrosymmetric space group. Figure 1 shows the complex with relative configuration R_{Ru} and olefin coordination through the *si* enantioface.

To rationalize the diastereoselective formation of **2a**, the stability of both diastereomers and the corresponding energy barrier for the isomerization process have been estimated theoretically (B3LYP/6-31G(d,p) +

(5) Gamasa, M. P.; Gimeno, J.; Gonzalez-Bernardo, C.; Martin-Vaca, B. M. *Inorg. Chim. Acta* **2003**, *347*, 181.
(6) Garrou, P. E. *Chem. Rev.* **1981**, *81*, 229.
(7) Eliel, E.; Wilen, S. H. *Stereochemistry of Organic Compounds*; Wiley: New York, 1994.
(8) (a) Okuda, J.; Zimmermann, K. H. *Chem. Ber.* **1989**, *122*, 1645. (b) Faller, J. W.; Johnson, B. V. *J. Organomet. Chem.* **1975**, *88*, 101. (c) Miguel-Garcia, J. A.; Adams, H.; Maitlis, P. M. J. *J. Organomet. Chem.* **1991**, *413*, 427.
(9) (a) Barthel-Rosa, L. P.;. Maitra, K.; Nelson, J. H. *Inorg. Chem.* **1998**, *37*, 633. (b) This is in contrast to the dissociative mechanism proposed for the derivative [Ru(η^5-C_5Me_5){κ^3(*P,C,C*)-$Ph_2P(CH_2CR{=}CH_2)$}{κ^1(*P*)-$Ph_2P(CH_2CH{=}CH_2)$}][PF_6], in which a coordinatively unsaturated intermediate is required. However, no theoretical calculations have been performed with this system.
(10) Similar dynamic proceses have been described for other metal complexes: (a) Clark, P. W.; Hanisch, P.; Jones, A. J. *Inorg. Chem.* **1979**, *18*, 2067. (b) Clark, P. W.; Jones, A. J. *J. Organomet. Chem.* **1976**, *122*, C41. See also ref 8c.

Scheme 2. B3LYP/6-31G(d,p) + LANL2DZ DH Values Including Solvent Effects

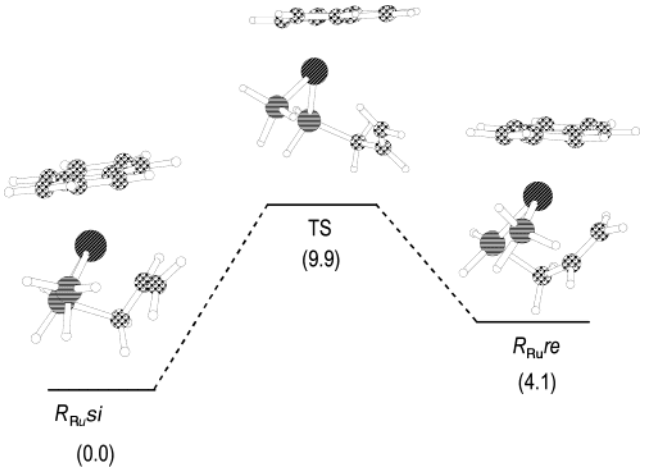

LANL2DZ level). Scheme 2 shows the energy profile for the interconversion between the $R_{Ru}si$ and $R_{Ru}re$ conformers of the model compound $[Ru(\eta^5\text{-}C_9H_7)\{\kappa^3(P,C,C)\text{-}PH_2(C_3H_5)\}(PH_3)]^+$ used to carry out the calculations, and the most representative geometrical parameters for the $R_{Ru}si$ and $R_{Ru}re$ diastereomers as well as the transition structures connecting them are shown in Figure 2. The thermodynamic parameters as computed at the different levels of theory employed can be found in the Supporting Information. The geometry of the $R_{Ru}si$ model compound is consistent with the experimental X-ray data (see Figure 1).

The theoretical calculations indicate a single-step mechanism for the interconversion between the $R_{Ru}si$ and $R_{Ru}re$ diastereomers, involving an 18e species in which the double bond remains coordinated to ruthenium.[11] The calculated rotation barrier is relatively low (9.9 kcal/mol), which would favor the existence of a fast equilibrium between the two diastereomers. However, the variable-temperature NMR spectra of complexes **2a**,**b** reveal the absence of a dynamic process involving the coordination of both diastereotopic faces of the olefin. This may be due to the relative stability of the isomers, which has been estimated to be 4.4 kcal/mol in the model system and which is likely to become even larger in complexes **2**, due to the larger steric requirements arising from the presence of both indenyl and phenyl groups in the ruthenium fragment $[Ru(\eta^5\text{-}C_9H_7)\{\kappa^3\text{-}(P,C,C)\text{-}PPh_2(C_3H_5)\}(PPh_3)]$. A large difference in relative stability would preclude the detection of the second isomer and yield the observed enantiofacial chiral recognition. Steric hindrance would also raise the energy barrier for interconversion. Recent theoretical calculations including explicitly phenyl groups on similar half-sandwich ruthenium complexes[12] do confirm such expectations. However, the huge computational effort required in the present case prevented us from making a quantitative exploration of the steric effects.

(11) Alternatively, Gladysz has proposed a mechanism for the interconversion of both diastereomers in the complexes $[Re(\eta^5\text{-}C_5H_5)(NO)(PPh_3)(H_2C{=}CHR)][BF_4]$ which proceeds also without alkene dissociation involving a carbon−hydrogen σ-bond. However, no theoretical calculations have been performed. Peng, T.-S.; Gladysz, J. A. *J. Am. Chem. Soc.* **1992**, *114*, 4174.

(12) Braña, P.; Gimeno, J.; Sordo, J. A. *J. Org. Chem.*, in press.

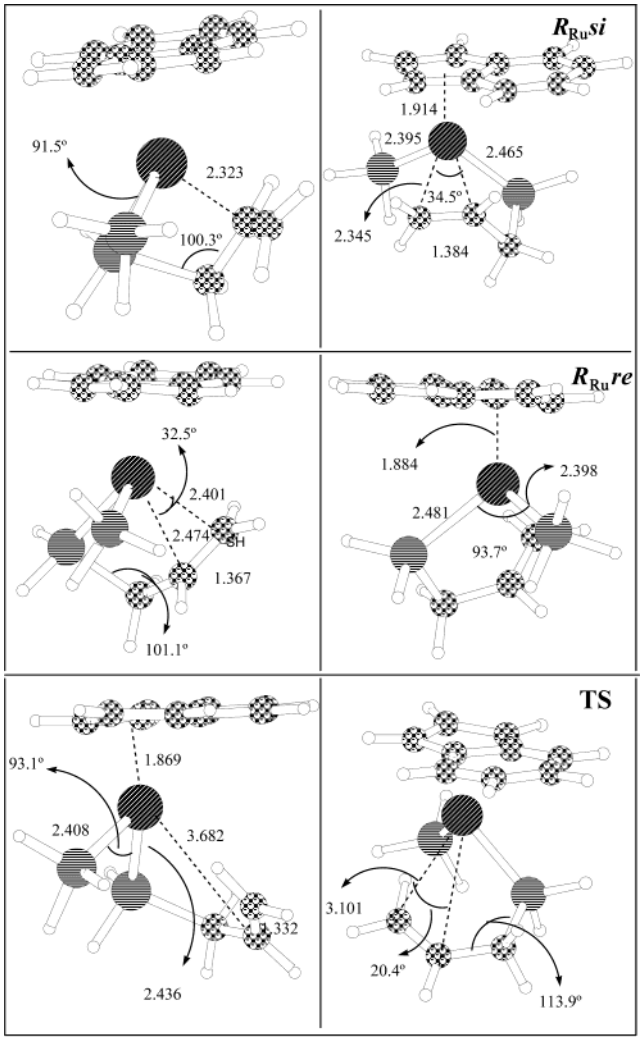

Figure 2. Geometrical parameters for the structures located on the PES as computed at the B3LYP level using the 6-31G(d,p) basis set and the LANL2DZ pseudopotential.

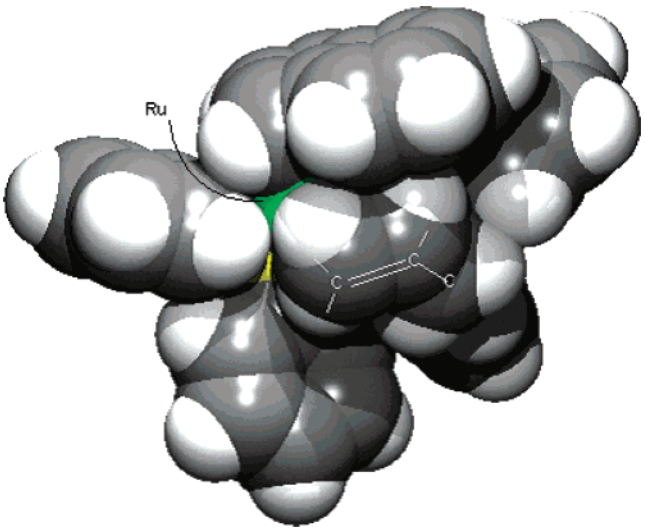

Figure 3. Space-filling representation for complex **2a**.

The space-filling representation of the crystal structure of complex **2a** shown in Figure 3 is in accordance with the steric effects, indicating that the space around atom C_β is limited by the indenyl ring and the phenyl groups. This highly congested space probably makes the

motion required for the interconversion process described in Scheme 2 much more difficult from an energetic viewpoint (higher value of the TS energy).

Reactivity of the Complexes [Ru(η^5-C_9H_7){κ^3-(*P,C,C*)-$Ph_2P(CH_2CR{=}CH_2)$}(PPh_3)][PF_6] (R = H (2a), Me (2b)) toward Nucleophiles. To study the propensity of the coordinated π-olefinic system to undergo nucleophilic addition, due to its electrophilic character, or to behave as a leaving group in substitution reactions, we have explored the reactivity of complexes **2a** and **2b** toward typical neutral and anionic two-electron species such as nitriles, hydride, azide or alkyl carbanions.

(a) π-Olefin Exchange Reactions: Synthesis of the Cationic [Ru(η^5-C_9H_7){κ^1(*P*)-$Ph_2P(CH_2CR{=}CH_2)$}(PPh_3)L][PF_6] (R = H, L = MeCN (3a), BzCN (3b)) and Neutral [Ru(η^5-C_9H_7)(N_3){κ^1(*P*)-$Ph_2P(CH_2CR{=}CH_2)$}(PPh_3)] (R = H (4a), Me (4b)) Complexes. Substitution of the coordinated π-olefin group is achieved readily by refluxing a solution of complex **2a** and either one of the nitriles RC≡N (R = Me, Bz) in CH_2Cl_2 (1:1.5 molar ratio), yielding the complexes **3a**,**b** (80%). Similarly, the addition of NaN_3 to a THF/MeOH solution of **2a**,**b** at room temperature results in the formation of the neutral complexes [Ru(η^5-C_9H_7)(N_3)-{κ^1(*P*)-$Ph_2P(CH_2CRCH_2)$}(PPh_3)] (R = H (**4a**), Me (**4b**)) as orange solids in 80−90% yield.

Complexes **3a**,**b** and **4a**,**b** have been characterized by elemental analysis and IR and NMR spectroscopy, and the results obtained are in agreement with the proposed formulations (see Experimental Section for details). Thus, the $^{31}P\{^1H\}$ NMR spectra show the two doublet resonances for the AB system at δ 49.0 and 44.1 (d, J_{PP} = 36.6 Hz) (**3a**), δ 49.4 and 42.6 (J_{PP} = 36.6 Hz) (**3b**), δ 46.5 and 50.8 (d, J_{PP} = 41.5 Hz) (**4a**), and δ 46.7 and 51.3 (J_{PP} = 41.1 Hz) (**4b**), values which are in agreement with those found for complexes **1a**,**b**, in which the allylphosphine acts as a monodentate ligand. The coordination of the azide ligands to the metal center was confirmed by IR spectroscopy, which shows the typical ν(N−N) bands at 2003 cm^{-1} (**4a**) and 2007 cm^{-1} (**4b**).

(b) Nucleophilic Additions: Synthesis of the Complexes [Ru(η^5-C_9H_7){κ^2(*P,C*)-Ph_2P{$CH_2C(R)(Nu)CH_2$}}(PPh_3)] (R = H, Nu = Me (5a), *n*Bu (5b), H (5c); R = Me, Nu = Me (6a), *n*Bu (6b), H (6c)). The treatment of THF solutions of complexes **2a**,**b** with lithium carbanions R′Li (R′ = Me, *n*Bu), at room temperature results in the regioselective addition at the internal C_β atom of the coordinated allylic group to afford the ruthenaphosphacyclopentane complexes [Ru{κ^2(*P,C*)-Ph_2P{$CH_2C(R)(R')CH_2$}}(η^5-C_9H_7)(PPh_3)] (R = H, R′ = Me (**5a**), *n*Bu (**5b**); R = Me, R′ = Me (**6a**), *n*Bu (**6b**)). Similarly, complexes **2a** and **2b** react with Li[$B(C_2H_5)_3H$] to give, regioselectively, the analogous addition products [Ru{κ^2(*P,C*)-Ph_2P{$CH_2CH(R)CH_2$}}(η^5-C_9H_7)(PPh_3)] (R = H (**5c**), Me (**6c**)). Complexes **5a**−**c** and **6a**−**c** have been isolated as air-stable orange solids in 80−95% yield after chromatographic workup.

Analytical and NMR (^1H, $^{31}P\{^1H\}$, and $^{13}C\{^1H\}$) spectroscopic data of **5a**−**c** and **6a**−**c** support the proposed formulations (see the Experimental Section for details), in which a regioselective addition at the β-carbon atom of the coordinated allyl group has occurred. Significantly, NMR spectra of **5a**,**b** and **6a**,**c** prove that the additions also proceed in a stereoselective manner, since only one diastereomer is obtained in each case. This is readily assessed by the $^{31}P\{^1H\}$ NMR spectra, which display only two doublet resonances at δ 58.6−61.6 and 61.5−71.3 (see Experimental Section). Other significant spectroscopic features are (i) the $^{13}C\{^1H\}$ NMR spectra (see Experimental Section), which display the carbon atom CR(R′) signal as a doublet resonance at δ 31.8−49.0 (J_{CP} = 6.8−19.1 Hz) (DEPT experiments), and (ii) the ^1H and $^{13}C\{^1H\}$ NMR spectra, which show the typical CH_2 resonances in the ranges δ 0.86−2.98 ppm (CH_2) and 15.4−43.3 (CH_2) as expected for sp^3 carbon nuclei (see Experimental Section). It is worth mentioning that complexes **5a** and **6c**, resulting from the additions of methyllithium and hydride to the π-olefin complexes **2a** and **2b**, respectively, are diastereomers, as expected from the diastereotopic coordination of the olefin in the precursors.

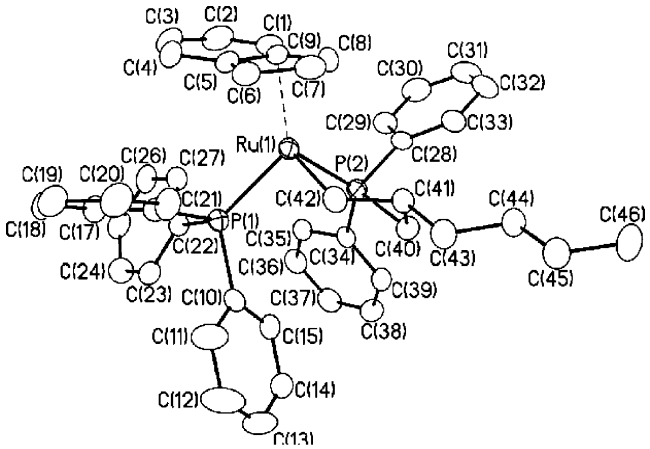

Figure 4. Molecular structure and atom-labeling scheme for one molecule of complex **5b**. Non-hydrogen atoms are represented by their 50% probability ellipsoids. Hydrogen atoms have been omitted for clarity. Selected bond lengths (Å): Ru(1)−C* = 1.9405(19), Ru(1)−P(1) = 2.2823(11), Ru(1)−P(2) = 2.2719(12), Ru(1)−C(42) = 2.131(4), P(2)−C(40) = 1.843(4), C(40)−C(41) = 1.523(6), C(41)−C(42) = 1.532(6). Selected bond angles (deg): C*−Ru(1)−P(1) = 127.46(7), C*−Ru(1)−P(2) = 125.62(8), C*−Ru(1)−C(42) = 117.30(14), P(1)−Ru(1)−P(2) = 101.54(4), P(1)−Ru(1)−C(42) = 88.55(12), P(2)−Ru(1)−C(42) = 81.65(13), Ru(1)−P(2)−C(40) = 105.00(15), P(2)−C(40)−C(41) = 106.4(3). C(40)−C(41)−C(42) = 107.9(3), Ru(1)−C(42)−C(41) = 110.6(3). C* = centroid of the indenyl ligand.

Since the stereochemistry of the new chiral carbon atoms was not revealed by the NMR data, a single-crystal X-ray structure determination was carried out for the complex **5b**. An ORTEP view of the molecular geometry is shown in Figure 4. Selected bond distances and angles are collected in the caption.

The asymmetric unit consists of two molecules of complex **5b**, which differ significantly in the conformation of the butyl chain but which are essentially identical in all other aspects. Since the relevant structural parameters are similar, only those corresponding to one molecule will be discussed.[13] The structure shows the following: (i) The molecule exhibits a pseudooctahedral three-legged piano-stool geometry with the η^5-indenyl ligand displaying the usual allylene coordination mode with bonding parameters comparable to those of others

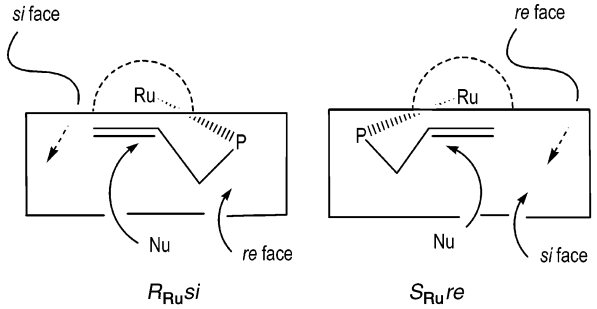

Figure 5. Nucleophilic attacks on each of the enantiomers of complex **2a**.

reported by us previously.[14] It is interesting to note that the benzo ring of the indenyl ligand is located between the two phosphorus atoms of the phosphines, resulting in a formally trans orientation with respect to the Ru−C(42) σ-bond. (ii) The skeleton of the metallaphosphacycle shows conventional single-bond distances (P(2)−C(40), C(41)−C(40), C(42)−C(41), and Ru(1)−C(42)). The torsion angle P(2)−C(40)−C(41)−C(42) is 50.4(4)°, and the conformational helical chirality is δ. (iii) The relative configurations of the new stereogenic carbon atom C(41) and the ruthenium atom are $R_{Ru}S_C$. The other enantiomer $S_{Ru}R_C$ is present in equal proportion in the crystal.

As expected, the addition occurs on the C=C face opposite the ruthenium, generating a new stereogenic C_β atom. The observed relative configuration *S*, for the stereoisomer with absolute configuration *R* at Ru, results from exo attack on the *re* face of the olefin in the diastereomer $R_{Ru}si$ (relative configuration *R* at the C_β carbon atom results from exo attack on the *si* face of the enantiomer $S_{Ru}re$ of the starting olefin; Figure 5).

This fact is also in accord with the formation of the two diastereomers [Ru(η^5-C_9H_7){κ^2(*P*,*C*)-$Ph_2PCH_2C(Me)HCH_2$}(PPh_3)] (**6c** and **5a**), arising from the exo addition of hydride and methyl anions to complexes **2b** and **2a,** respectively. This also rules out the alternative mechanism involving exchange of the coordinated olefin by hydride and subsequent insertion of the allyl group into the Ru−H bond. In fact, all attempts to promote insertion reactions in the hydride complex [Ru(η^5-C_9H_7)H{κ^1(*P*)-$Ph_2PCH_2CH{=}CH_2$}(PPh_3)] (**1c**) have been unsuccessful.

Kinetic Studies. Hemilabile ligands containing weakly coordinating carbon moieties and, in particular, the olefins are of special interest, due to the well-known lability of the metal−olefin bond, which enables the facile generation of a free coordination site at the metal center. In particular, only a few ruthenium derivatives containing chelated alkenylphosphines have been described: i.e., [Ru(η^5-C_5Me_5){κ^1(*P*)-$Ph_2PCH{=}CH_2$}{κ^3(*P*,*C*,*C*)-$Ph_2PCH{=}CH_2$}][PF_6],[15] [Ru(η^5-C_5Me_5){κ^1(*P*)-$Ph_2PCH_2CH{=}CH_2$}{κ^3(*P*,*C*,*C*)-$Ph_2PCH_2CH{=}CH_2$}][PF_6],[9a] and [RuTpCl{κ^3(*P*,*C*,*C*)-$Ph_2PCH{=}CHCR{=}CH_2$}][16] (Tp = tris(pyrazolyl)borate). We have recently reported that complexes **2a**,**b** react rapidly with terminal alkynes to give the vinylidene complexes [Ru(η^5-C_9H_7)(=C=C(H)R){κ^1(*P*)-$Ph_2PCH_2CH{=}CH_2$)}(PPh_3)][PF_6],[17] in which the allylphosphine has become monodentate. Analogous behavior is also observed in the formation of [Ru(η^5-C_5Me_5){κ^1(*P*)-$Ph_2PCH_2CH{=}CH_2$)}$_2$L][PF_6] from [Ru(η^5-C_5Me_5){κ^1(*P*)-$Ph_2PCH_2CH{=}CH_2$}{κ^3(*P*,*C*,*C*)-$Ph_2PCH_2CH{=}CH_2$}][PF_6], which occurs readily through exchange of the coordinated olefin by two-electron ligands.[9a]

The ligand exchange reactions of complex **2a** in the presence of neutral nitriles, MeCN and BzCN, with formation of the cationic complexes **3a**,**b**, clearly indicate the hemilabile character of the allylphosphine ligand. Since no mechanistic studies have been reported on these exchange processes to date, we have investigated the kinetics of the reaction of complex **2a** with acetonitrile. In a series of $^{31}P\{^1H\}$ NMR spectra for the reaction with MeCN (0.375 M), in $CDCl_3$ at 38 °C, the low-frequency peak at δ −69.9 ppm of complex **2a** (0.0013 M) decreases exponentially until it disappears completely, with quantitative transformation into the two doublet resonances of complex **3a**. Intermediate species were not detected during the measurements. A plot of $\ln[\mathbf{2a}]_t/[\mathbf{2a}]_0$ (see Supporting Information), which is linear up to 93% of reaction corresponding to 4 half-lives, $t_{1/2}$, yields a value of the observed rate constant, $k_{obs} = 0.0016\ s^{-1}$. When the same process is observed by ^1H NMR, using CD_3CN as reagent, the disappearance of the peak at δ 5.42 ppm, due to the H-2 proton of the indenyl ligand, can be followed conveniently and peak integration gives the concentration values of **2a** at different times. The first-order analysis yields a value of k_{obs} which is the same, within experimental error, as that obtained in the $^{31}P\{^1H\}$ NMR experiment.

Since the reaction is first-order in complex **2a**, the dependence on the reagent has been investigated by a series of kinetic experiments, performed by ^1H NMR, at different CD_3CN concentrations. A plot of k_{obs} values vs [CD_3CN] is shown in Figure 6. The dependence of k_{obs} on the concentration of deuterated acetonitrile is linear, the slope of the line corresponding to the value of the second-order rate constant, $k_2 = [4.2(\pm0.1)] \times 10^{-3}\ M^{-1}\ s^{-1}$. In addition, the plot identifies a positive intercept on the *y* axis, which indicates a contribution to k_{obs} independent of [CD_3CN] and only first-order in complex **2a**, with a value of $[1.5(\pm0.6)] \times 10^{-4}\ s^{-1}$.

This is a classic case in the chemical kinetics of transition-metal complexes, described by eq 1, which implies the presence of parallel second- and first-order routes, more specifically of an associative pathway, in which both complex and reagent participate in the rate-limiting step (k_2), and of a dissociative pathway, in which a step involving ligand dissociation is rate limit-

(13) The stereochemistry of the chiral centers is identical qualitatively and practically identical quantitatively in the two molecules of a given asymmetric unit; for example, the chiral volumes calculated for the chiral carbon atoms C41 and C87 are equal in sign and nearly equal in magnitude.

(14) (a) Cadierno, V.; Díez, J.; Gamasa, M. P.;. Gimeno, J.; Lastra, E. *Coord.. Chem. Rev.* **1999**, *193−195*, 147. (b) Cadierno, V.; Gamasa, M. P.; Gimeno, J.; Gonzalez-Cueva, M.; Lastra, E.; Borge, J.; Pérez-Carreño, E.; García-Granda, S. *Organometallics* **1996**, *15*, 2137. (c) Cadierno, V.; Conejero, S.; Gamasa, M. P.; Gimeno, J.; Pérez-Carreño, E.; García-Granda, S. *Organometallics* **2001**, *20*, 3175.

(15) Barthel-Rosa, L. P.; Maitra, K.; Fischer, J.; Nelson, J. H. *Organometallics* **1997**, *16*, 1714.

(16) (a) Slugovc, C.; Mauthner, K.; Mereiter, K.; Schmid, R.; Kirchner, K. *Chem. Eur. J.* **1998**, *4*, 2043. (b) Slugovc, C.; Wiede, P.; Mereiter, K.; Schmid, R.; Kirchner, K. *Organometallics* **1997**, *16*, 2768.

(17) Alvarez, P.; Lastra, E.; Gimeno, J.; Bassetti, M.; Falvello, L. R. *J. Am. Chem. Soc.* **2003**, *125*, 2386.

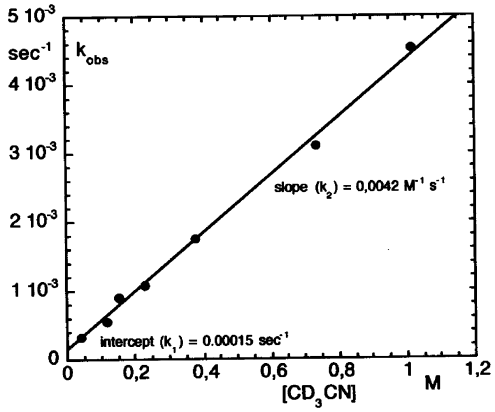

Figure 6. Plot of k_{obs} values vs [MeCN-d_3], for the reaction of complex **2a**, in $CDCl_3$ at 38 °C.

ing (k_1).[18] Substitution reactions via dissociative path-

$$k_{obs} = k_1 + k_2[CD_3CN] \quad (1)$$

ways have been described for indenyl complexes. This is the case for phosphine substitution in the ruthenium complex [RuCl(η^5-C_9H_7)(PPh_3)$_2$], yielding chiral-at-metal complexes [RuCl(η^5-C_9H_7)(PPh_3)(L′)],[19] or carbonyl substitution in the iron complex [FeI(η^5-C_9H_7)(CO)$_2$].[20] These dissociative routes do not involve η^3 intermediates. Mixed associative and dissociative mechanisms are also known, as in the case of [WCl(η^5-C_9H_7)(CO)$_3$].[21]

In the present case, the dissociative step is followed by fast reaction with CD_3CN, resulting in zero-order dependence on this reagent. A contribution from the solvent to the acetonitrile-independent pathway is unlikely, due to the negligible nucleophilic character of $CDCl_3$.[22]

The kinetic behavior of the reaction of complex **2a** with acetonitrile-d_3 is interesting, in light of the bonding modes of the allylphosphine complex and of the intramolecular nature of the leaving group in the substitution process. The substitution of the allylic double bond by the neutral donor ligand occurs preferentially via a rate-determining associative step[23] (k_2 route of eq 1 and Scheme 3). This pathway may involve the formation of an η^3-indenyl intermediate,[24] in which the ring slippage from the η^5 coordination of the substrate would facilitate the accommodation of the nitrile reagent in the ruthenium coordination sphere, and assist the olefin decoordination in a subsequent rapid step. This picture

Scheme 3

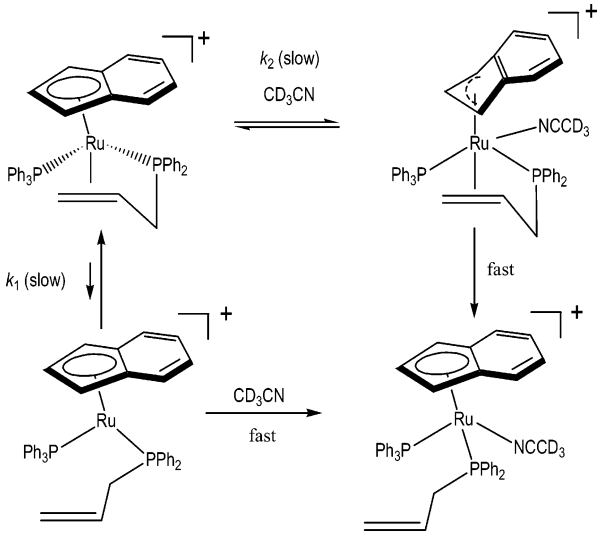

conforms with the mechanism described for the insertion reaction of alkynes into the metal−hydrogen bond of the indenylruthenium complex [RuH(η^5-C_9H_7)(dppm)].[3b,25] The associative pathway of ligand substitution reactions, characterized by second-order kinetics, is the classic route followed by transition-metal indenyl complexes,[26] as in the seminal case of carbonyl substitution by PPh_3 in the complex [Rh(η^5-C_9H_7)(CO)$_2$].[27]

The interesting feature of the reactivity of complex **2a** is the presence of parallel associative and dissociative routes. The k_1 value represents the rate of olefin dissociation from ruthenium to yield a reactive 16-electron, coordinatively unsaturated complex. This species, due to its highly reactive character, can form only as a transient, in competition between reversal to substrate by double-bond recoordination and attack of the neutral nitrile to form the product. In analogy to the intramolecular ligand dissociative pathway proposed for complex **2a**, the diastereomeric equilibration observed for the bis(allylphosphine) complex [Ru(η^5-C_5Me_5){κ^1(*P*)-$Ph_2PCH_2CH{=}CH_2$}{κ^3(*P*,*C*,*C*)-$Ph_2PCH_2CH{=}CH_2$}][PF_6] as well as its substitution reactions have been proposed to proceed via a dissociative mechanism involving the allylic double bond.[9a]

The overall mechanistic features of the ligand substitution process in complex **2a** are described in Scheme 3.[28] One special feature of this study is therefore the kinetic detection of the hemilabile character of an allylphosphine ligand, a finding which is unprecedented.

Conclusions

In this work the synthesis of diastereoselectively pure indenyl complexes [Ru(η^5-C_9H_7){κ^3(*P*,*C*,*C*)-$Ph_2P(CH_2$-$CR{=}CH_2$)}(PPh_3)][PF_6] is reported. These products be-

(18) Atwood, J. D. *Inorganic and Organometallic Reaction Mechanisms*; Brooks/Cole: Monterey, CA, 1985; p 131.

(19) Gamasa, M. P.; Gimeno, J.; Gonzalez-Bernardo, C.; Martín-Vaca, B.; Monti, D.; Bassetti, M. *Organometallics* **1996**, *15*, 302.

(20) Jones, D. J.; Mawby, R. J. *Inorg. Chim. Acta* **1972**, *6*, 157−160.

(21) Turaki, N. N.; Huggins, J. M.; Lebioda, L. *Inorg. Chem.* **1988**, *27*, 424−427.

(22) The existence of the dissociative equilibrium of the allylphosphine ligand from the κ^3 coordinating mode to the monodentate species, and its role in the reactivity of complex **2a**, indicated by κ^1, should be independent of the reagent or of the specific reaction. Accordingly, the reaction of complex **2a** with phenylacetylene, yielding vinylidene complexes,[17] also proceeds by mixed first- and second-order pathways and identifies a similar value of κ^1, under the same experimental conditions of solvent and temperature. Alvarez, P.; Bassetti, M.; Gimeno, J.; Lastra, E. Unpublished results.

(23) Olefin substitution by two-electron ligands is also observed for C_5Me_5 complexes.[9] Although no kinetic studies have been carried out for this reaction, a dissociative pathway has been proposed.

(24) (a) Calhorda, M. J.; Veiros, L. F. *Coord. Chem. Rev.* **1999**, *185−186*, 37. (b) O'Connor, J. M.; Casey, C. P. *Chem. Rev.* **1987**, *87*, 307.

(25) Bassetti, M.; Casellato, P.; Gamasa, M. P.; Gimeno, J.; Gonzalez-Bernardo, C.; Martín-Vaca, B. *Organometallics* **1997**, *16*, 5470.

(26) (a) Bang, H.; Lynch, T. J.; Basolo, F. *Organometallics* **1992**, *11*, 40. (b) Foo, T.; Bergman, R. G. *Organometallics* **1992**, *11*, 1811. (c) Bonifaci, C.; Carta, G.; Ceccon, A.; Gambaro, A.; Santi, S. *Organometallics* **1996**, *15*, 1630.

(27) Rerek, M. E.; Basolo, F. *J. Am. Chem. Soc.* **1984**, *106*, 5908.

(28) A similar kinetic and mechanistic analysis has been recently reported for the oxidative addition reaction of methyl iodide to a cationic rhodium(I) complex of a hemilabile tridentate S,N,S ligand (Bassetti, M.; Capone, A.; Salamone, M. *Organometallics* **2004**, *23*, 247).

long to a very scarce series of chiral-at-metal semisandwich complexes in which an effective chiral recognition of a prochiral allyl group has been achieved.[1] Other examples with high thermodynamic binding selectivities are very rare, i.e. [RuH(η^6-arene)(PR_3)(styrene)][SbF_6] (R = Ph, OMe),[29] although in solution the configurational diastereomers rapidly interconvert at low temperature.[30] Crystallographic data and theoretical calculations support both ruthenium and olefin configurations. Estimated values of the thermodynamic stabilities found in both diastereomers are in agreement with the experimentally observed enantioface binding selectivity. The enantiofacial selectivity can be also established on the basis of steric requirements, in which the phenyl groups of both phosphines may generate a "chiral pocket" for the allyl group, allowing formation of one of the diastereomers. Exchange processes of the coordinated olefin group in the complex [Ru(η^5-C_9H_7){κ^3-(*P*,*C*,*C*)-$Ph_2P(CH_2CR{=}CH_2)$}(PPh_3)][PF_6] by two-electron ligands reveal the hemilabile properties of the allylphosphine. Kinetic studies on the substitution reaction of complex **2a** with a nitrile ligand indicate that the olefin exchange occurs via parallel first-order (dissociative) and second-order (associative) pathways and highlight the involvement of a transient coordinatively unsaturated species. This represents an unprecedented kinetic detection of the hemilabile character of an allylphosphine ligand. The capacity of the metal fragment for the coordination of just one of the diastereotopic olefin faces has permitted the study of nucleophilic additions, which proceed regioselectively on the *exo* face, giving rise to chiral ruthenacyclopentane rings. In summary, we have developed a ruthenium fragment which is able to act as a Lewis acid with chiral recognition, providing an appropriate means to envisage potential enantioselective transformations of prochiral olefins and similar unsaturated substrates. Further work devoted to exploring the scope of this ability will be undertaken.

Experimental Section

General Considerations. All manipulations were performed under an atmosphere of dry nitrogen using vacuum-line and standard Schlenk techniques. All reagents were obtained from commercial suppliers and used without further purification. Solvents were dried by standard methods and distilled under nitrogen before use. The compounds [Ru(η^5-C_9H_7)Cl(PPh_3)$_2$][31] and $Ph_2P(C_3H_5)$[32] were prepared by previously reported methods. Infrared spectra were recorded on a Perkin-Elmer 1720-XFT or a Perkin-Elmer 599 IR spectrometer. The C, H, and N analyses were carried out with a Perkin-Elmer 240-B microanalyzer. NMR spectra were recorded on Bruker AC300 and 300DPX instruments at 300 MHz (^{1}H), 121.5 MHz (^{31}P), or 75.4 MHz (^{13}C) using $SiMe_4$ or 85% H_3PO_4 as standards. DEPT experiments were carried out for all the compounds. Coupling constants *J* are given in hertz. Abbreviations used: Ar, aromatic; s, singlet; d, doublet; vt, virtual triplet; m, multiplet. The following atom labels have been used for the ^{1}H and ^{13}C{^{1}H} spectroscopic data:

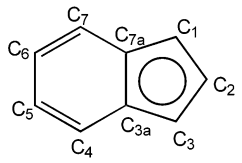

Theoretical Calculations. Density functional theory (DFT) calculations at the B3LYP level[33] were carried out in order to explore the potential energy surface (PES) of the model compound [Ru(η^5-C_9H_7){κ^1(*P*)-$PH_2(CH_2CHCH_2)$}(PH_3)]$^+$. The LANL2DZ effective core potential[34] was chosen for Ru and P, while the standard 6-31G(d,p) basis sets[35] were employed for the rest of the atoms. Experience has shown that this level of theory provides reasonable predictions for transition-metal-containing compounds.[36] Graphical analysis of the imaginary frequencies of the transition structures as well as intrinsic reaction coordinate (IRC)[37] calculations allowed us to interconnect the different structures located on the PES and then construct the energy profiles.

Solvation effects were estimated by performing single-point calculations with the self-consistent reaction field (SCRF) Onsager model.[38] A dielectric constant of 8.93 (corresponding to dichloromethane) solute and radii of 5.30, 5.28, and 5.04 Å were employed to emulate the solvent effects through single-point calculations on R_{Ru}*si*, TS, and R_{Ru}*re* , respectively. Further optimizations, including solvent effects, on the R_{Ru}*si* and R_{Ru}*re* species were also accomplished in order to analyze the role played by the solvent on the optimized geometries. Two figures in the Supporting Information show the rather small influence of the solvent on the geometrical parameters.

Thermochemical corrections for the liquid phase were not included. The thermodynamic functions were estimated within the ideal gas, rigid rotor, and harmonic oscillator approximations.[39] The Gaussian 98 package of programs[40] was used to carry out the calculations. A temperature of 298.15 K and a pressure of 1 atm were assumed.

Synthesis of [Ru(η^5-C_9H_7)Cl{κ^1(*P*)-$Ph_2P(CH_2C(R)CH_2)$}(PPh_3)] (R = H (1a), Me (1b)). A mixture of [Ru(η^5-C_9H_7)Cl(PPh_3)$_2$] (0.77 g, 1 mmol) and the corresponding allyldiphen-

(29) Faller, J. W.; Chase, K. J. *Organometallics* **1995**, *14*, 1592.

(30) Analogous chiral ruthenium complexes containing either η^1(O)-bonded or η^2(C=C)-bonded methylacrylate and other enal ligands have been described: (a) Carmona, D.; Cativiela, C.; Elipe, S.; Lahoz, F. J.; Lamata, M. P.; López-Ram de Viu, M. P.; Oro, L. A.; Vega, C.; Viguri, F. *J. Chem. Soc., Chem. Commun.* **1997**, 2351. (b) Kundig, E. P.; Saudan, C. M.; Alezra, V.; Viton, F.; Bernardinelli, G. *Angew. Chem., Int. Ed.* **2001**, *40*, 4481. (c) Motoyama, Y.; Kurihara, O.; Murata, K.; Aoki, K.; Nishiyama, H. *Organometallics* **2000**, *19*, 1025.

(31) Oro, L. A.; Ciriano, M. A.; Campo, M.; Foces-Foces, C.; Cano, F. H. *J. Organomet. Chem.* **1985**, *289*, 117.

(32) Clark, P. W.; Curtis, J. L. S.; Garrou, P. E.; Hartwell, G. E. *Can. J. Chem.* **1974**, *52*, 1714.

(33) Cramer, C. S. *Essentials of Computational Chemistry: Theories and Models*, Wiley: New York, 2002.

(34) (a) Hay, P. J.; Wadt, W. R. *J. Chem. Phys.* **1985**, *82*, 270. (b) Wadt, W. R.; Hay, P. J. *J. Chem. Phys.* **1985**, *82*, 284. (c) Hay, P. J.; Wadt, W. R. *J. Chem. Phys.* **1985**, *82*, 299.

(35) Hehre, W. J.; Radom, L.; Schleyer, P. v. R.; Pople, J. A. *Ab Initio Molecular Orbital Theory*; Wiley: New York, 1986.

(36) *Chem. Rev.* **2000**, *100*, 351−818. The whole issue is devoted to computational transition-metal chemistry.

(37) (a) González, C.; Schlegel, H. B. *J. Chem. Phys.* **1989**, *90*, 2154. (b) González, C.; Schlegel, H. B. *J. Chem. Phys.* **1990**, *94*, 5523.

(38) (a) Wong, M. W.; Frisch, M. J.; Wiberg, K. B. *J. Am. Chem. Soc.* **1991**, *113*, 4776. (b) Wong, M. W.; Wiberg, K. B.; Frisch, M. J. *J. Am. Chem. Soc.* **1992**, *114*, 523.

(39) McQuarrie, D. A. *Statistical Thermodynamics*; University Science Books: Mill Valley, CA, 1973.

(40) Frisch, M. J.; Trucks, G. W.; Schlegel, H. B.; Scuseria, G. E.; Robb, M. A.; Cheeseman, J. R.; Zakrzewski, V. G.; Montgomery, J. A., Jr.; Stratmann, R. E.; Burant, J. C.; Dapprich, S.; Millam, J. M.; Daniels, A. D.; Kudin, K. N.; Strain, M. C.; Farkas, O.; Tomasi, J.; Barone, V.; Cossi, M.; Cammi, R.; Mennucci, B.; Pomelli, C.; Adamo, C.; Clifford, S.; Ochterski, J.; Petersson, G. A.; Ayala, P. Y.; Cui, Q.; Morokuma, K.; Malick, D. K.; Rabuck, A. D.; Raghavachari, K.; Foresman, J. B.; Cioslowski, J.; Ortiz, J. V.; Stefanov, B. B.; Liu, G.; Liashenko, A.; Piskorz, P.; Komaromi, I.; Gomperts, R.; Martin, R. L.; Fox, D. J.; Keith, T.; Al-Laham, M. A.; Peng, C. Y.; Nanayakkara, A.; Gonzalez, C.; Challacombe, M.; Gill, P. M. W.; Johnson, B. G.; Chen, W.; Wong, M. W.; Andres, J. L.; Head-Gordon, M.; Replogle, E. S.; Pople, J. A. *Gaussian 98*, revision A.6; Gaussian, Inc.: Pittsburgh, PA, 1998.

ylphosphine (1.1 mmol) in thf (25 mL) was refluxed for 10 min. The solution was evaporated to dryness to afford a red solid, which was washed with hexane (20 mL) and vacuum-dried. The excess of PPh_3 was eliminated by sublimation at 80 °C on a high-vacuum pump. R = H (**1a**): yield 85%; $^{31}P\{^1H\}$ NMR (121.5 MHz, $CDCl_3$): δ 48.0 (d, J_{PP} = 43.0 Hz), 45.3 (d, J_{PP} = 43.0 Hz); ^1H NMR (300 MHz, $CDCl_3$) δ 1.85 (m, 1H, CH_2), 3.32 (m, 1H, CH_2), 3.03 (s br, 1H, =CH_2), 4.40 (s, 1H, H1), 4.57 (s, 1H, H3), 4.92 (m, 1H, =CH_2), 4.85 (s, 1H, H2), 4.87 (m, 1H, =CH), 6.3−7.7 (m, 24H, ArH); $^{13}C\{^1H\}$ NMR (75.4 MHz, $CDCl_3$) δ 30.8 (d, J_{CP} = 21.7 Hz, CH_2), 64.1 (s, C1), 71.8 (d, J_{CP} = 11.5 Hz, C3), 92.9 (s, C2), 112.2, 113.8 (both s, C3a, C7a), 119.8 (d, J_{CP} = 8.5 Hz, =CH_2), 125.8, 126.8 (both s, C4,5,6,7), 128.1 (s, =CH), 129.3−139.6 (m, Ar). Anal. Calcd for $C_{42}H_{37}ClP_2Ru$ (740.2): C, 68.15; H, 5.04. Found: C, 68.01; H, 5.21. R = Me (**1b**): yield 85%; $^{31}P\{^1H\}$ NMR (121.5 MHz, $CDCl_3$) δ 48.8 (d, J_{PP} = 42.2 Hz), 45.5 (d, J_{PP} = 42.2 Hz); ^1H NMR (300 MHz, $CDCl_3$) δ 0.89 (s, 3H, CH_3), 1.80 (dd, J_{PH} = 15.7 Hz, J_{HH} = 8.3 Hz, 1H, CH_2), 2.94 (s, 1H, =CH_2), 3.39 (dd, J_{PH} = 15.7 Hz, J_{HH} = 8.3 Hz, 1H, CH_2), 4.04 (s, 1H, H2), 4.28 (s, 1H, =CH_2), 4.79 (s, 2H, H1,3), 6.3−7.7 (m, 24H, Ar H); $^{13}C\{^1H\}$ NMR (75.4 MHz, $CDCl_3$) δ 24.5 (s, CH_3), 30.3 (d, J_{CP} = 17.4 Hz, CH_2), 61.6 (s, C1), 69.8 (d, J_{CP} = 11.6 Hz, C3), 90.8 (s, C2), 109.6, 111.0 (both s, C3a, C7a), 115.2 (d, J_{CP} = 7.5 Hz, =CH_2), 123.3, 124.9 (both s, C4,5,6,7), 129.3−139.6 (m, Ar), 140.1 (d, J_{CP} = 13.9 Hz, =CCH_3). Anal. Calcd for $C_{43}H_{39}ClP_2Ru$ (754.2): C, 68.47; H, 5.21. Found: C, 68.51; H, 5.03.

Synthesis of [Ru(η^5-C_9H_7)H{κ^1(*P*)-$Ph_2P(C_3H_5)$}(PPh_3)] (1c). A solution of [Ru(η^5-C_9H_7)Cl{κ^1(*P*)-$Ph_2P(C_3H_5)$}(PPh_3)] (**1a**; 0.74 g, 1 mmol) and NaOMe (1 mmol) in MeOH (25 mL) was refluxed for 30 min. Once the solution was cooled, the resulting solid was recovered by filtration, washed with hexane (2 × 10 mL), and dried under vacuum. Yield: 80%. $^{31}P\{^1H\}$ NMR (121.5 MHz, C_6D_6): δ 66.2 (d, J_{PP} = 25.9 Hz, PPh_3), 53.3 (d, J_{PP} = 25.9 Hz, ADPP). ^1H NMR (300 MHz, C_6D_6): δ −15.32 (vt, $^2J_{HP}$ = 31.9 Hz, hydride), 1.98 (m, 2H, CH_2), 2.79 (m, 1H, =CH_2), 2.84 (m, 1H, =CH_2), 4.18 (m, 1H, CH), 5.31 (s, 1H, H1), 5.36 (s, 1H, H2) 5.52 (s, 1H, H3), 6.25 (m, 2H, C_9H_7), 6.99−7.83 (m, 27H, Ar H)). $^{13}C\{^1H\}$ NMR (75.4 MHz, C_6D_6): δ 31.1 (s br, CH_2), 79.6 (s, C1), 80.8 (s, C3), 91.13 (s, C2), 105.5 (s, C3a), 105.3 (s, C7a), 114.4 (s br, =CH_2), 118.2 (s br, =CH), 125.9−136.2 (m, Ar). Anal. Calcd for $C_{42}H_{38}P_2Ru$ (705.8): C, 71.48; H, 5.43. Found: C, 71.03; H, 5.59.

Synthesis of [Ru(η^5-C_9H_7){κ^3(*P,C,C*)-$Ph_2PCH_2C(R)CH_2$}(PPh_3)][PF_6] (R = H (2a), Me (2b)). A solution of the complex [Ru(η^5-C_9H_7)Cl{κ^1(*P*)-$Ph_2P(CH_2C(R)CH_2)$}(PPh_3)] (R = H (**1b**), Me (**1b**); 1 mmol) in MeOH (25 mL) was treated with $NaPF_6$ (0.16 g, 1 mmol), and the mixture was refluxed for 30 min. The solution was evaporated to dryness. The resulting solid was extracted with dichloromethane (2 × 20 mL) and vacuum-dried to give the desired complexes as yellow solids. R = H (**2a**): yield 90%; $^{31}P\{^1H\}$ NMR (121.5 MHz, $CDCl_3$) δ 55.2 (d, J_{PP} = 36.6 Hz, PPh_3), −69.9 (d, J_{PP} = 36.6 Hz, ADPP); ^1H NMR (300 MHz, $CDCl_3$) δ 1.98 (m, 2H, CH_2), 2.79 (m, 1H, =CH), 2.84 (m, 1H, =CH_2), 4.18 (vt, 1H, J_{HH} = 10.6 Hz, =CH_2), 4.78 (s, 1H, H1), 5.36 (s, 1H, H3) 5.42 (s, 1H, H2), 6.25 (m, 2H, C_9H_7), 6.99−7.83 (m, 27H, Ar H); $^{13}C\{^1H\}$ NMR (75.4 MHz, $CDCl_3$) δ 31.1 (s br, CH_2), 54.4 (d, J_{CP} = 20.6 Hz, =CH), 58.2 (s br, =CH_2), 79.6 (s, C1), 80.8 (s, C2), 91.1 (s, C3), 105.5 (s, C3a), 105.3 (s, C7a), 125.9−136.2 (m, Ar). Anal. Calcd for $C_{42}H_{37}F_6P_3Ru$ (849.7): C, 59.37; H, 4.39. Found: C, 59.12; H, 4.42. R = Me (**2b**): yield 90%; $^{31}P\{^1H\}$ NMR (121.5 MHz, $CDCl_3$) δ 51.4 (d, J_{PP} = 34.5 Hz, PPh_3), −63.9 (d, J_{PP} = 34.5 Hz, ADPP); ^1H NMR (300 MHz, $CDCl_3$) δ 1.97 (s, 1H, CH_3), 2.14 (m, 2H, CH_2), 2.69 (d, 1H, J_{PH} = 15.09 Hz, =CH_2), 4.18 (vt, 1H, J_{PH} = 13.1 Hz, =CH_2), 4.55 (s, 1H, H1), 5.29 (s, 1H, H3), 5.86 (s, 1H, H2), 6.05 (m, 2H, C_9H_7), 6.99−7.83 (m, 27H, Ar H); $^{13}C\{^1H\}$ NMR (75.4 MHz, $CDCl_3$) δ 26.8 (s, CH_3), 35.5 (d, J_{CP} = 34.5 Hz, CH_2), 55.8 (s br, =CH_2), 67.5 (d, J_{CP} = 18.0 Hz, =CCH_3), 76.8 (s, C1), 77.6 (s, C2), 92.2 (s, C3), 104.3 (s, C3a), 110.3 (s, C7a), 121.6−136.8 (m, Ar). Analytically pure samples of this compound could not be obtained.

Synthesis of [Ru(η^5-C_9H_7)(NCR){κ^1(*P*)-$Ph_2PCH_2CHCH_2$}(PPh_3)][PF_6] (R = Me (3a), Bz (3b)). To a solution of [Ru(η^5-C_9H_7){κ^3(*P,C,C*)-$Ph_2PCH_2CHCH_2$}(PPh_3)] (**2a**; 0.85 g 1 mmol) in CH_2Cl_2 (25 mL) was added RCN (1.5 mmol), and the solution was refluxed for 45 min. After it was cooled, the solution was evaporated to dryness and the solid residue was recrystallized from CH_2Cl_2, washed with diethyl ether (2 × 10 mL), and vacuum-dried. R = Me (**3a**): yield 85%; $^{31}P\{^1H\}$ NMR (121.5 MHz, $CDCl_3$) δ 49.0 (d, J_{PP} = 36.6 Hz), 44.1 (d, J_{PP} = 36.6 Hz); ^1H NMR (300 MHz, $CDCl_3$) δ 2.21 (m, 1H, CH_2), 2.31 (s, 3H, CH_3), 2.42 (m, 1H, CH_2), 3.56 (s, 1H, =CH_2), 4.48 (m, 1H, =CH_2), 4.86 (m, 1H, H1), 4.91 (m, 1H, H3), 5.01 (m, 1H, H2), 5.26 (m, 1H, =CH), 6.71−7.61 (m, 29H, Ar H); $^{13}C\{^1H\}$ NMR (75.4 MHz, $CDCl_3$) δ 46.4 (s br, CH_2), 66.6 (s, C1), 70.0 (s, C3), 94.1 (s, C2), 101.2 (s, C3a), 103.2 (s, C7a), 119.3 (s br, =CH_2), 123.6 (s br, =CH),125.5−136.4 (m, Ar), 137.9 (s, CN); IR (Nujol) ν 2226 cm^{-1} (CN). Anal. Calcd for $C_{44}H_{40}NF_6P_3Ru$ (890.8): C, 59.33; H, 4.53. Found: C, 59.19; H, 4.43. R = Bz (**3b**): yield 85%; $^{31}P\{^1H\}$ NMR (121.5 MHz, $CDCl_3$) δ 49.4 (d, J_{PP} = 36.6 Hz), 42.6 (d, J_{PP} = 36.6 Hz); ^1H NMR (300 MHz, $CDCl_3$) δ 2.40 (m, 1H, CH_2), 2.51 (m, 1H, CH_2), 3.70 (s, 1H, =CH_2), 4.32 (m, 1H, H1), 4.63 (m, 1H, H2), 4.96 (m, 1H, H3), 5.22 (m, 1H, =CH_2), 5.37 (m, 1H, =CH), 6.43−7.67 (m, 34H, Ar H); $^{13}C\{^1H\}$ NMR (75.4 MHz, $CDCl_3$) δ 31.9 (d, J_{CP} = 21.1 Hz, CH_2), 66.6 (s, C1), 70.0 (s, C2), 94.1 (s, C3), 101.7 (s, C3a), 104.1 (s, C7a), 119.6 (s br, =CH_2), 123.9 (s br, =CH), 125.5−136.4 (m, Ar), 141.3 (s, CN); IR (Nujol) ν 2224 cm^{-1} (CN). Anal. Calcd for $C_{50}H_{44}NF_6P_3Ru$ (966.9): C, 62.11; H, 4.59. Found: C, 62.40; H, 4.88.

Synthesis of [Ru(η^5-C_9H_7)(N_3){κ^1(*P*)-$Ph_2P(CH_2C(R)CH_2)$}(PPh_3)] (R = H (4a), Me (4b)). To a solution of [Ru(η^5-C_9H_7)Cl{κ^1(*P*)-$Ph_2P(CH_2C(R)CH_2)$}(PPh_3)] (R = H (**1a**), Me (**1b**); 1 mmol) in THF/MeOH (10:1; 20 mL) was added dropwise a solution of NaN_3 (0.06 g, 1 mmol, in 2 mL of MeOH). The solution was stirred for 2 h at room temperature. The resulting solid was filtered, and the solution was evaporated to dryness to afford a red solid, which was purified by column chromatography by recovery of the fraction eluted with diethyl ether and evaporation to dryness. R = H (**4a**): yield 90%; $^{31}P\{^1H\}$ NMR (121.5 MHz, $CDCl_3$) δ 46.5 (d, J_{PP} = 41.5 Hz), 50.8 (d, J_{PP} = 41.5 Hz); ^1H NMR (300 MHz, $CDCl_3$) δ 1.88 (m, 1H, CH_2), 2.80 (m, 1H, CH_2), 3.16 (s, 1H, =CH_2), 4.38 (s, 1H, H2), 4.60 (m, 1H, =CH_2), 4.79 (s, 2H, H1, H3), 4.81 (m, 1H, =CH), 6.3−7.7 (m, 29H, Ar H); $^{13}C\{^1H\}$ NMR (75.4 MHz, $CDCl_3$) δ 30.0 (d, J_{CP} = 20.8 Hz, CH_2), 62.5 (s, C1), 67.4 (d, J_{CP} = 11.1 Hz, C3), 90.3 (s, C2), 109.0, 110.2 (both d, J_{CP} = 3.3 Hz, C3a, C7a), 117.6 (d, J_{CP} = 8.5 Hz, =CH_2), 122.4 (d, J_{CP} = 14.8 Hz, =CH), 127.3−137.5 (m, Ar); IR (Nujol) ν 2003 cm^{-1} (N_3). Analytically pure samples of this compound could not be obtained. R = Me (**4b**): yield 80%; $^{31}P\{^1H\}$ NMR (121.5 MHz, $CDCl_3$) δ 46.7 (d, J_{PP} = 41.1 Hz), 51.3 (d, J_{PP} = 41.1 Hz); ^1H NMR (300 MHz, $CDCl_3$) δ 1.03 (m, 3H, CH_3), 1.87 (m, 1H, CH_2), 1.93 (m, 1H, CH_2), 4.19 (s, 1H, H2), 4.32 (s, 1H, =CH_2), 4.59 (m, 1H, =CH_2), 4.32 (s, 2H, H1, H3), 6.3−7.7 (m, 29H, Ar H); $^{13}C\{^1H\}$ NMR (75.4 MHz, $CDCl_3$) δ 15.25 (s, CH_3), 32.2 (d, J_{CP} = 17.5 Hz, CH_2), 62.5 (s, C1), 67.8 (d, J_{CP} = 11.0 Hz, C3), 90.8 (s, C2), 109.0, 110.2 (both d, J_{CP} = 4.0 Hz, C3a, C7a), 115.6 (d, J_{CP} = 7.5 Hz, =CH_2), 122.7 (d, J_{CP} = 15.6 Hz, =CH), 127.4−141.5 (m, Ar); IR (Nujol) ν 2007 cm^{-1} (N_3). Anal. Calcd for $C_{43}H_{39}N_3P_2Ru$ (760.8): C, 67.88; H, 5.17. Found: C, 67.39; H, 5.40.

Synthesis of [Ru(η^5-C_9H_7){κ^2(*P,C*)-$Ph_2PCH_2CR(R')CH_2$}(PPh_3)] (R = H, R' = Me (5a), *n*Bu (5b), H (5c); R = Me, R' = Me (6a), *n*Bu (6b), H (6c)). A stirred solution of [Ru(η^5-C_9H_7){κ^3(*P,C,C*)-$Ph_2P(CH_2C(R)CH_2)$}(PPh_3)][PF_6] (R = H (**2a**), Me (**2b**); 1 mmol) in THF (10 mL) at room temperature was treated dropwise with MeLi (**5a**, **6a**), *n*BuLi (**5b**, **6b**) or LiB(C_2H_5)$_3$H (**5c**, **6c**) (2 mol). The solution immediately turned orange. After 10 min, the solvents were evaporated to dryness

and the resulting solid was extracted with dichloromethane (20 mL) and vacuum-dried. The filtrate was washed with hexane (3 × 20 mL), and the solvents were removed under vacuum. The solid obtained was purified by column chromatography by recovery of the fraction eluted with diethyl ether. R = H, R' = Me (**5a**): yield 85%; $^{31}P\{^1H\}$ NMR (121.5 MHz, C_6D_6) δ 61.5 (d, J_{PP} = 29.3 Hz), 60.0 (d, J_{PP} = 29.3 Hz); ^1H NMR (300 MHz, C_6D_6) δ 1.16 (m, 1H, CH_2), 1.41 (d, J_{HH} = 5.9 Hz, 3H, Me), 1.47 (m, 1H, CH_2), 2.28 (m, 1H, CH_2), 2.71 (m, 1H, CH_2), 2.85 (m, 1H, CH), 4.22 (s, 1H, H1), 4.35 (s, 1H, H3), 5.08 (s, 1H, H2), 6.54−7.91 (m, 29H, Ar H); $^{13}C\{^1H\}$ NMR (75.4 MHz, C_6D_6) δ 14.6 (s, Me), 23.9 (s, CH_2), 31.8 (d, J_{CP} = 6.8 Hz, CH), 37.9 (d, J_{CP} = 30.5 Hz, CH_2), 71.9 (d, J_{CP} = 9.0 Hz, C1), 77.5 (d, J_{CP} = 8.9 Hz, C3), 97.2 (s, C2), 105.0 (s, C3a, C7a), 111.0 (s, C3a, C7a), 120.7 (s, C_9H_7), 121.2 (s, C_9H_7), 123.9−148.6 (m, Ar). Anal. Calcd for $C_{43}H_{40}P_2Ru$ (719.8): C, 71.75; H, 5.60. Found: C, 70.61; H, 5.42. R = Me, R' = Me (**6a**): yield 80%; $^{31}P\{^1H\}$ NMR (121.5 MHz, C_6D_6) δ 63.4 (d, J_{PP} = 27.3 Hz), 61.2 (d, J_{PP} = 27.3 Hz); ^1H NMR (300 MHz, C_6D_6) δ 0.99 (m, 1H, CH_2), 1.31 (d, J_{HH} = 5.7 Hz, 3H, Me), 1.61 (d, J_{HH} = 6.0 Hz, 3H, Me), 1.92 (m, 1H, CH_2), 2.31 (m, 1H, CH_2), 3.07 (m, 1H, CH_2), 4.34 (s, 1H, H1), 4.55 (s, 1H, H3), 5.18 (s, 1H, H2), 6.64−7.89 (m, 29H, Ar H); $^{13}C\{^1H\}$ NMR (75.4 MHz, C_6D_6) δ 13.2 (s, Me), 15.8 (s, Me), 31.2 (s, CH_2), 35.3 (d, J_{CP} = 29.3 Hz, CH_2), 41.5 (d, J_{CP} = 15.3 Hz, $C(CH_3)_2$), 68.9 (d, J_{CP} = 7.9 Hz, C1), 76.4 (d, J_{CP} = 6.9 Hz, C3), 98.8 (s, C2), 110.0, 111.6 (both s, C3a, C7a), 122.7 (s, C_9H_7), 124.2 (s, C_9H_7), 129.1−149.6 (m, Ar). Anal. Calcd for $C_{44}H_{42}P_2Ru$ (733.8): C, 72.02; H, 5.77. Found: C, 73.01; H, 6.58. R = H, R' = *n*Bu (**5b**): yield 85%; $^{31}P\{^1H\}$ NMR (121.5 MHz, C_6D_6) δ 61.9 (d, J_{PP} = 29.1 Hz), 60.5 (d, J_{PP} = 29.1 Hz); ^1H NMR (300 MHz, C_6D_6) δ 0.88−1.77 (m, 11H, Me, CH_2), 1.99 (m, 1H, CH_2), 2.64 (m, 1H, CH_2), 2.78 (m, 1H, CH), 4.15 (s, 1H, H1), 4.28 (s, 1H, H3), 5.02 (s, 1H, H2), 6.51−7.69 (m, 29H, Ar H); $^{13}C\{^1H\}$ NMR (75.4 MHz, C_6D_6) δ 14.3 (s, Me), 18.4 (d, J_{CP} = 7.3 Hz, CH_2), 23.9 (s, CH_2), 31.8 (s, CH_2), 38.0 (d, J_{CP} = 30.5 Hz, CH_2), 40.4 (d, J_{CP} = 19.5 Hz, CH_2), 49.0 (d, J_{CP} = 17.0 Hz, CH), 71.8 (d, J_{CP} = 8.5 Hz, C1), 77.5 (d, J_{CP} = 8.5 Hz, C3), 97.2 (s, C2), 105.5 (s, C3a), 111.7 (s, C7a), 120.3 (s, C_9H_7), 123.4 (s, C_9H_7), 126.0−138.2 (m, Ar), 141.4 (d, J_{CP} = 30.5 Hz, Ph), 147.4 (d, J_{CP} = 32.7 Hz, Ph). Anal. Calcd for $C_{46}H_{46}P_2Ru$ (761.9): C, 72.52; H, 6.09. Found: C, 72.54; H, 5.88. R = Me; R' = *n*Bu (**6b**): yield 80%; $^{31}P\{^1H\}$ NMR (121.5 MHz, C_6D_6) δ 69.9 (d, J_{PP} = 21.3 Hz), 61.3 (d, J_{PP} = 21.3 Hz); ^1H NMR (300 MHz, C_6D_6) δ 0.86−1.90 (m, 12H, 2 CH_3, CH_2), 2.03 (m, 2H, CH_2), 2.98 (m, 1H, CH_2), 2.81 (m, 1H, CH_2), 4.01 (s, 1H, H1), 4.44 (s, 1H, H3), 5.14 (s, 1H, H2), 6.51−7.69 (m, 29H, Ar H); $^{13}C\{^1H\}$ NMR (75.4 MHz, C_6D_6) δ 11.2 (s, CH_3), 19.3 (s, CH_3), 20.9 (d, J_{CP} = 8.1 Hz, CH_2), 25.4 (s, CH_2), 30.8 (s, CH_2), 41.3 (d, J_{CP} = 19.1 Hz, *C*MeBu), 43.3 (d, J_{CP} = 29.6 Hz, CH_2), 51.4 (d, J_{CP} = 19.1 Hz, CH_2), 65.8 (d, J_{CP} = 10.9 Hz, C1), 75.4 (d, J_{CP} = 8.1 Hz, C3), 99.2 (s, C2), 105.5 (s, C3a), 112.3 (s, C7a), 118.4 (s, C_9H_7), 125.9 (s, C_9H_7), 127.0−140.4 (m, Ar), 145.3 (d, J_{CP} = 29.7 Hz, Ph) ppm. Anal. Calcd for $C_{47}H_{48}P_2Ru$ (775.9): C, 72.75; H, 6.24. Found: C, 73.01; H, 6.58. R = H; R' = H (**5c**): yield 95%; $^{31}P\{^1H\}$ NMR (121.5 MHz, C_6D_6) δ 71.3 (d, J_{PP} = 29.0 Hz), 61.6 (d, J_{PP} = 29.0 Hz); ^1H NMR (300 MHz, C_6D_6) δ 1.35 (m, 1H, CH_2), 1.51 (m, 1H, CH_2), 1.71 (m, 1H, CH_2), 2.34 (m, 1H, CH_2), 2.65 (m, 1H, CH_2), 2.98 (m, 1H, CH_2), 4.22 (s, 1H, H1), 4.49 (s, 1H, H3), 5.07 (s, 1H, H2), 6.61−7.61 (m, 29H, Ar H); $^{13}C\{^1H\}$ NMR (75.4 MHz, C_6D_6) δ 15.4 (s, CH_2), 32.4 (d, J_{CP} = 31.2 Hz, CH_2), 35.1 (s, CH_2), 72.0 (d, J_{CP} = 8.6 Hz, C1), 76.9 (d, J_{CP} = 8.8 Hz, C3), 96.9 (s, C2), 107.5 (s, C3a), 112.7 (s, C7a), 123.2 (s, C_9H_7), 123.7 (s, C_9H_7), 126.0−141.7 (m, Ar). Anal. Calcd for $C_{42}H_{38}P_2Ru$ (705.8): C, 71.48; H, 5.43. Found: C, 71.32; H, 5.58. R = Me; R'= H (**6c**): yield 85%; $^{31}P\{^1H\}$ NMR (121.5 MHz, C_6D_6) δ 64.6 (d, J_{PP} = 29.7 Hz), 58.6 (d, J_{PP} = 29.7 Hz); ^1H NMR (300 MHz, C_6D_6) δ 0.98 (m, 1H, CH_2), 1.18 (d, J_{HH} = 6.3 Hz, 3H, Me), 1.91 (m, 1H, CH_2), 2.15 (m, 2H, CH_2), 2.41 (m, 1H, CH), 4.31 (s, 1H, H1), 4.36 (s, 1H, H3), 5.01 (s, 1H, H2), 6.49−7.12 (m, 29H, Ar H); $^{13}C\{^1H\}$ NMR (75.4 MHz, C_6D_6) δ 11.2 (s, Me), 20.5 (d, J_{CP} = 6.0 Hz, CH_2), 37.0 (d, J_{CP} = 13.0 Hz, CH), 39.0 (d, J_{CP} = 30.7 Hz, CH_2), 73.8 (d, J_{CP} = 8.2 Hz, C1), 74.3 (d, J_{CP} = 7.7 Hz, C3), 97.1 (s, C2), 105.7 (s, C3a, C7a), 110.3 (s, C3a, C7a), 121.6−134.3 (m, C_9H_7, Ar). Anal. Calcd for $C_{43}H_{40}P_2Ru$ (719.8): C, 71.75; H, 5.60. Found: C, 71.58; H, 5.64.

Table 1. Crystal Data and Structure Refinement for 2a and 5b

	2a·CH_2Cl_2	**5b**
empirical formula	$C_{44}H_{41}Cl_4F_6P_3Ru$	$C_{46}H_{46}P_2Ru$
mol wt	1019.55	761.84
temp, K	150(2)	123(1)
wavelength, Å	0.710 73	0.710 73
cryst syst	monoclinic	triclinic
space group	$P2_1/c$	$P\bar{1}$
unit cell dimens		
a, Å	18.166(5)	10.0870(2)
b, Å	15.0807(18)	19.3200(5)
c, Å	17.655(6)	19.5780(5)
α, deg	90	86.7610(18)
β, deg	117.55(2)	83.9990(19)
γ, deg	90	78.4560(10)
V, Å^3	4288.2(19)	3715.23(15)
Z	4	4
calcd density, g cm^{-3}	1.579	1.362
abs coeff, mm^{-1}	0.786	0.540
F(000)	2064	1584
cryst size, mm	0.44 × 0.23 × 0.13	0.35 × 0.12 × 0.03
θ range for data collecn, deg	2.31−25.01	1.05−27.92
index ranges	$-21 \le h \le 19$, $-17 \le k \le 0$, $0 \le l \le 20$	$0 \le h \le 13$, $-24 \le k \le 25$, $-25 \le l \le 25$
no. of rflns collected	7816	46 023
no. of indep rflns	7533 (*R*(int) = 0.0495)	17 507 (*R*(int) = 0.0927)
max and min transmissn	0.824 and 0.792	1.099 and 0.917
no. of variables	540	883
final *R* index ($I > 2\sigma(I)$)	R1 = 0.0570, wR2 = 0.1274	R1 = 0.0603, wR2 = 0.1433
R index (all data)	R1 = 0.1148, wR2 = 0.1489	R1 = 0.1020, wR2 = 0.1656

X-ray Diffraction Study of Complexes 2a and 5b. Data for **2a** were gathered on a CAD-4 diffractometer equipped with an FR558 low-temperature device.[41] After preliminary determination of the orientation matrix, axial photos were used to verify the cell dimensions. Scan parameters for intensity data collection were optimized with reference to two-dimensional ($\omega-\theta$) scans of 11 reflections. During intensity data collection, a variable counting time was used, depending on the intensity measured in a rapid initial scan. The weakest reflections were measured at the slowest speed; none were skipped. Absorption corrections were based on nine ψ-scans of reflections with Eulerian angle χ between −30.3 and +49.8°.[42] For **5b** (the asymmetric unit contains two independent molecules), diffraction data were gathered using a Nonius KappaCCD four-circle diffractometer[41] equipped with an Oxford Cryosystems Model 600 cryostat. Integration of the 354 data frames was followed by application of the usual corrections, including absorption corrections.[42] Both structures were solved by direct methods[43] and refined by full-matrix least-squares calculations.[44] In **2a** the asymmetric unit included two formula equivalents of CH_2Cl_2, one ordered and one disordered; similarity restraints were used for the two congeners at the

(41) (a) CAD-4 control program: CAD4/PC, version 2.0; Nonius BV, Delft, The Netherlands, 1996. (b) KappaCCD control program: Collect; Nonius BV, Delft, The Netherlands, 1997−2000.

(42) (a) Data reduction for CAD4: Harms K.; Wocadlo, S. XCAD4B; 1995. (b) Absorption correction for CAD4: SHELXTL release 5.05/V; Siemens, 1996. (c) DENZO-SCALEPACK, data reduction for KappaCCD: Otwinowski, Z.; Minor, W. Processing of X-ray Diffraction Data Collected in Oscillation Mode. In *Macromolecular Crystallography, Part A*; Methods Enzymol. No. 276; Carter, C. W., Jr., Sweet, R. M., Eds.; Academic Press: New York, 1997; pp 307−326. (d) Absorption correction for KappaCCD-SORTAV:Blessing, R. H. *Acta Crystallogr., Sect. A* **1995**, *51*, 33.

disordered site. For both refinements hydrogen atoms were placed at calculated positions—including the methyl hydrogen atoms in **5b**, which were placed so as to give staggered conformations—and refined as riding atoms with isotropic displacement parameters assigned as 1.2 times the equivalent isotropic displacement parameters of their respective parent carbon atoms. Non-hydrogen atoms were refined anisotropically. The two refinements converged with the residuals given in Table 1.

Kinetic Measurements. A weighed amount of complex **2a** (11−13 mg) was dissolved in $CDCl_3$ (0.5 mL) in an NMR tube under argon, and the appropriate amount of MeCN-d_3 was added using a microsyringe. ^{31}P NMR (Bruker AC 300 P) or ^1H NMR spectra (Bruker AM 200) were collected immediately after mixing, allowing about 1 min for thermal equilibration and experiment setup and using a macro sequence. The temperature in the NMR probe was determined from the chemical shift difference between OH and CH_2 signals of a solution of ethylene glycol containing 20% DMSO-d_6.[45] The observed rate constants for consumption of complex **2a** (k_{obs}, s^{-1}) were obtained from nonlinear least-squares regression analysis by fitting the exponential dependence of concentration, *c*, calculated *via* peak intensities for ^{31}P, or peak integration for ^1H, against time, according to the first-order rate equation: $C_t = C_\infty + (C_0 - C_\infty)\exp(-k_{obs}t)$. The procedure yields values of c_∞, k_{obs}, and the correlation coefficient. The k_{obs} values were checked against those obtained from straight-line plots of ln *c vs* time.

Acknowledgment. This work was supported by the Spanish MCT (Project Nos. 1FD97-0565, BQU2000-0227, BQU-3660-C02-01, and BQU2002-00554) and Working Group D24/0014/02 of COST CHEMISTRY Action D24.

Supporting Information Available: Tables giving B3LYP/6-31G(d,p) + LANL2DZ absolute energy values, thermodynamic data, and Cartesian coordinates for the computed structures, two figures showing optimized structures including solvent effects ($\epsilon = 9.83$) and a $\ln[\mathbf{2a}]_t/[\mathbf{2a}]_0$ plot, a table of kinetic rate constants, and tables giving crystallographic data for **2a** and **5b**. This material is available free of charge via the Internet at http://pubs.acs.org. Crystallographic data are also available from the Cambridge Crystallographic Data Centre (CCDC-210218 (**2a**) and CCDC-210219 (**5b**)).

OM040001Q

(43) (a) For **2a**: Sheldrick, G. M. SHELXS-97: FORTRAN Program for Crystal Structure Solution; University of Göttingen, Göttingen, Germany, 1997. (b) For **5b**: Beurskens, P. T.; Beurskens, G.; Bosman, W. P.; de Gelder, R.; Garcia-Granda, S.; Gould, R. O.; Israel, R; Smits, J. M. M. DIRDIF96 Program System; Crystallography Laboratory, University of Nijmegen, Nijmegen, The Netherlands, 1996.

(44) Sheldrick, G. M. SHELXL-97: FORTRAN Program for Crystal Structure Refinement; University of Göttingen, Göttingen, Germany, 1997.

(45) Van Geet, A. L. *Anal. Chem*. **1968**, *40*, 2227.